HHS Public Access

Author manuscript

Eur Radiol. Author manuscript; available in PMC 2022 May 01.

Published in final edited form as:

Eur Radiol. 2021 May ; 31(5): 2778–2787. doi:10.1007/s00330-020-07386-4.

Diagnostic Accuracy of Non-Contrast Quiescent Interval Slice-Selective (QISS) MRA Combined with MRI-based Vascular Calcification Visualization for the Assessment of Arterial Stenosis in Patients with Lower-Extremity Peripheral Artery Disease

Akos Varga-Szemes, MD, PhD[1], **Megha Penmetsa, MD**[1], **Tilman Emrich, MD**[1,2,3], **Thomas M. Todoran, MD**[4], **Pal Suranyi, MD, PhD**[1], **Stephen R. Fuller, BS**[1], **Robert R. Edelman, MD**[5,6], **Ioannis Koktzoglou, PhD**[5,7], **U. Joseph Schoepf, MD**[1]

[1]Division of Cardiovascular Imaging, Department of Radiology and Radiological Science, Medical University of South Carolina, Charleston, SC

[2]Department of Diagnostic and Interventional Radiology, University Medical Center of the Johannes Gutenberg-University, Mainz, Germany

[3]German Centre for Cardiovascular Research, Partner site Rhine-Main, Mainz, Germany

[4]Division of Cardiology, Department of Medicine, Medical University of South Carolina, Charleston, SC

[5]Department of Radiology, NorthShore University, Evanston, IL

Address for Correspondence: U. Joseph Schoepf, MD, Division of Cardiovascular Imaging, Department of Radiology and Radiological Science, Medical University of South Carolina, Ashley River Tower, MSC 226, 25 Courtenay Dr, Charleston, SC 29425, Phone: 843-876-7146; Fax: 843-876-3182; schoepf@musc.edu.

Compliance with Ethical Standards

2. Guarantor:

The scientific guarantor of this publication is U. Joseph Schoepf.

4. Statistics and Biometry:

One of the authors has significant statistical expertise.

5. Informed Consent:

Only if the study is on human subjects:

Written informed consent was obtained from all subjects (patients) in this study.

6. Ethical Approval:

Institutional Review Board approval was obtained.

7. Study subjects or cohorts overlap:

n/a

8. Methodology

Methodology:

- prospective
- diagnostic or prognostic study
- performed at one institution

[6]Northwestern University Feinberg School of Medicine, Chicago, IL

[7]University of Chicago Pritzker School of Medicine, Chicago, IL

Abstract

Objectives: The proton density-weighted, in-phase stack-of-stars (PDIP-SOS) MRI technique provides calcification visualization in peripheral artery disease (PAD). This study sought to investigate the diagnostic accuracy of a combined non-contrast quiescent-interval slice-selective (QISS) MRA and PDIP-SOS MRI protocol for the detection of PAD, in comparison with CTA and digital subtraction angiography (DSA).

Methods: Twenty-six prospectively enrolled PAD patients (70±8 years) underwent lower extremity CTA and 1.5T or 3T PDIP-SOS/QISS MRI prior to DSA. Two readers rated image quality and graded stenosis (≥50%) on QISS MRA without/with calcification visualization. Sensitivity, specificity, and area under the curve (AUC) were calculated against DSA. Calcification was quantified and compared between MRI and non-contrast CT (NCCT) using paired t-test, Pearson's correlation and Bland-Altman analysis.

Results: Image quality ratings were significantly higher for CTA compared to MRA (4.0 [3.0–4.0] and 3.0 [3.0–4.0]; p=0.0369). The sensitivity and specificity of QISS MRA, QISS MRA with PDIP-SOS, and CTA for ≥50% stenosis detection were 85.4%, 92.2%, 90.2% and 90.3%, 93.2%, 94.2%, respectively, while AUCs were 0.879, 0.928, and 0.923, respectively. A significant increase in AUC was observed when PDIP-SOS was added to the MRA protocol (p=0.0266). Quantification of calcification showed significant differences between PDIP-SOS and NCCT (80.6±31.2mm^3 vs 88.0±29.8mm^3; p=0.0002) with high correlation (r=0.77, p<0.0001) and moderate mean of differences (−7.4mm^3).

Conclusion: QISS MRA combined with PDIP-SOS MRI provides improved, CTA equivalent, accuracy for the detection of PAD, although its image quality remains inferior to CTA.

Keywords

Peripheral artery disease; Magnetic resonance imaging; Vascular calcification; Computed tomography angiography; Non-contrast magnetic resonance angiography

Introduction

With an increasing number of patients being diagnosed with diabetes and hyperlipidemia, the prevalence of peripheral artery disease (PAD) has risen to 12% to 14% in the general population, and it further increases with age [1; 2]. Symptomatic patients usually undergo Doppler studies and ankle brachial index (ABI) assessment to diagnose the disease. Once PAD is diagnosed and a vascular intervention is potentially necessary, it is beneficial to obtain advanced imaging of the lower extremity vascular anatomy for treatment planning.

Both computed tomography angiography (CTA) and MR angiography (MRA) techniques can be used when outlining revascularization strategies [3]. An advantage of CTA over MRA is its ability to visualize arterial wall calcifications, although blooming artifacts in calcified areas may influence the assessment of stenosis significance [4]. However, neither CTA nor

MRA is without risk. The use of iodinated and gadolinium-based contrast materials can be a particular concern in PAD patients with comorbidities and poor renal function [3], especially in view of contrast-induced nephropathy [5], nephrogenic systemic fibrosis, and gadolinium deposition [6]. The current American College of Radiology guideline indicates that an estimated glomerular filtration rate of <30 ml/min/1.73 m^2 cut off should be used to identify patients who are at the highest risk of developing iodine contrast-induced nephropathy [7]. The use of the same threshold is recommended to avoid the administration of Group I gadolinium based contrast agents to reduce the risk for nephrogenic systemic fibrosis. As nearly 40% of patients with PAD have significant renal dysfunction [8], contrast administration in this patient group can be challenging.

The contrast media-related concerns along with technological advances have increased the interest in non-contrast MRA approaches. The non-contrast quiescent interval slice-selective (QISS) MRA technique has been introduced for the imaging of the lower extremity arterial system [9] and shows high diagnostic accuracy for the detection of significant vascular stenosis in PAD [10–13]. However, similarly to other MRA techniques, QISS MRA is unable to visualize vascular calcification. A recently introduced proton density-weighted, in-phase stack-of-stars (PDIP-SOS) gradient-echo prototype MR imaging (MRI) pulse sequence, however, seems to be promising for the accurate depiction and quantification of vascular calcifications in patients with PAD [14; 15]. It has also been shown that the PDIP-SOS technique provides similar performance in the ilio-femoral arteries regardless of the field strength (1.5T and 3T) [15].

In this study, we aimed to investigate the diagnostic accuracy of a combined non-contrast QISS MRA and PDIP-SOS MRI protocol for the detection of PAD, in comparison with CTA and digital subtraction angiography (DSA) as a reference.

Materials and Methods

Patient selection

The Institutional Review Board of the Medical University of South Carolina approved the protocol of this HIPAA compliant study and written informed consent was obtained from all patients. Consecutive PAD patients (n=26) who were referred for a clinically indicated lower extremity CTA for the evaluation of known or suspected PAD prior to DSA, were prospectively enrolled for a research MRI at 1.5T or 3T between February 2017 and January 2019. General MRI exclusion criteria were applied. The MRA and CTA were usually scheduled for the same day, but no more than 25 days apart; and within 40 days prior to DSA. The first author had full access to all the data in the study and takes responsibility for its integrity and the data analysis.

MR protocol

MR acquisitions were performed on 1.5T (MAGNETOM Avanto Dot, syngo VD13A, Siemens) and 3T (MAGNETOM Skyra Fit, syngo VE11C, Siemens) systems. Patients were placed feet first in a supine position. Body, peripheral and spine matrix phased-array radiofrequency coils were used for signal reception.

Non-contrast QISS MRA acquisition—QISS MRA was performed as an automated "push-button" protocol using an electrocardiographically-gated prototype pulse sequence as previously described [10]. The acquisition included eight to ten stations with 48 slices in each (144 mm z-axis coverage per station) to cover the entire run-off from the abdominal aorta to the feet. Imaging was performed without breathing commands except in the upper pelvis and abdominal regions. Typical pulse sequence parameters used at 1.5T and 3T are shown in Table 1. Following the completion of the protocol, maximum intensity projection (MIP) images were generated and briefly reviewed by an investigator with 11 years of experience in cardiovascular imaging to determine the positioning of the PDIP-SOS acquisition.

PDIP-SOS MRI acquisition—Based on the QISS MRA MIP, one or two areas of the run-off with the most severe PAD was chosen for the evaluation of vessel calcification. The prototype PDIP-SOS acquisition [14] was used with the pulse sequence parameters shown in Table 1. Typically 660 radial views were acquired in each slice-encoding step.

CTA protocol

A 3rd generation dual source CT system (SOMATOM Definition Force, Siemens) in dual energy mode was used for CTA image acquisition according to clinical protocols, including a topogram and a non-contrast CT scan (NCCT) followed by a CT angiogram. Images covered the region from the distal abdominal aorta down to the distal lower extremities. Patients received a total of 80 ml of intravenously administered iodinated contrast material (350 mgI/ml iohexol, GE Healthcare) by a multiphasic injection using an automated dual syringe power injector (Stellant D CT Injection System, Medrad) in accordance with current guidelines [16]. The CTA acquisition was timed based on a 120 kV bolus tracking approach (Care-Bolus, Siemens) and was performed applying the following parameters: FOV 350 mm; pitch 0.7; collimation, 2 × 64 × 0.6 mm for both detectors; and tube voltage and current, 150 kV/59 reference mAs for tube A and 90 kV/95 reference mAs for tube B. A soft tissue convolution kernel (Qr49, Siemens) with a section thickness of 1.5 mm and increment of 1.0 mm, and third generation advanced modeled iterative reconstruction algorithm (ADMIRE, Siemens) at a strength level of 3 (available strength level range 1 to 5) were used to reconstruct the data.

DSA protocol

DSA was used as the reference modality in this investigation. Of note, the performing operator (an interventional cardiologist with 15 years of experience in peripheral angiography) was aware of the CTA results, which were used for invasive procedure planning. DSA studies were performed through the transfemoral approach using a cardiovascular imaging system (Axiom Artis, Siemens). Contrast media (350 mgI/ml iohexol or 320 mgI/ml iodixanol, GE Healthcare) was delivered using a 5 F Omni Flush catheter (Angiodynamics). DSA was acquired using either the stepping-table technique in which the diagnostic catheter was placed in the distal abdominal aorta and both legs were imaged with a single power injection or selective angiography. Selective angiography was performed by first placing a catheter in the distal abdominal aorta to image the distal aorta, common iliac, external iliac and common femoral arteries. The catheter was then advanced

to the contralateral common femoral artery for additional imaging of the contralateral lower extremity. Imaging of the ipsilateral leg was then performed by retrograde injection through the common femoral artery sheath. Postero-anterior projections, with additional 30° left and 30° right anterior oblique views at the level of the iliac and common femoral arteries were acquired.

Image analysis

MR and CT image assessments were performed by two independent readers with 5 and 11 years of experience in cardiovascular imaging. All MR and CT angiograms were available to review as axial images, multiplanar reconstructions and coronal MIPs on dedicated workstations (Leonardo and syngo.via, Siemens). PDIP-SOS MRI datasets were displayed as source images, inverted minimum intensity projection images, and curved multi-planar reformats. The readers first evaluated all QISS MRA datasets without access to the PDIP-SOS data in a random order. After an interval of 14 days, the readers reevaluated the QISS MRA datasets along with PDIP-SOS-based visualization of intravascular calcification in a random order.

Finally, after an additional 14 days, the readers performed the assessment of CTA images in random order. DSA static and cine images were reviewed on a picture archive and communication system (IMPAX 6.5, AGFA Healthcare) by the interventional cardiologist. Vascular assessment was performed on a per-segment basis according to an 18-segment model [17].

Image quality and diagnostic confidence assessment—The per-segment image quality was rated in QISS MRA and CTA datasets on a 4-point Likert-scale as follows: (1) non-diagnostic image quality due to severe image artifacts and/or poor vascular signal, inadequate for diagnosis; (2) fair image quality with major artifacts and/or inhomogeneous vascular signal, acceptable for diagnosis; (3) good image quality with minor artifacts and/or moderately homogenous vascular signal, adequate for confident diagnosis; and (4) excellent image quality without artifacts and homogenous vascular signal, highly confident diagnosis. Quality scores 2 to 4 were considered acceptable for diagnostic purposes. A similar Likert-scale was used for PDIP-SOS MRI and NCCT: (1) severe image artifacts, inadequate for evaluation; (2) fair image quality with major artifacts, acceptable for evaluation; (3) good image quality with minor artifacts, adequate for evaluation; and (4) excellent image quality without artifacts.

Diagnostic accuracy—Intraluminal diameter stenosis was graded dichotomously (non-significant stenosis <50%; significant stenosis ≥50%) on a per-segment basis with all modalities. In case of multiple arterial stenoses in a single arterial segment, only the stenosis with the highest grade was considered. While the entire run-off was assessed on QISS-MRA and CTA, only segments with PDIP-SOS and DSA correlation were included in further diagnostic accuracy analysis.

Calcium quantification—NCCT and PDIP-SOS MRI datasets were co-localized based on vascular landmarks (e.g. femoral artery bifurcation) and vascular calcification was

quantified in the corresponding vessel segments. The volume of vessel wall calcification was measured segment by segment using an ImageJ (National Institutes of Health, Bethesda, MD) [18] based script as previously described [14]. Briefly, seed points were manually placed to define the centerline and length of the vessel segment, and calcification was quantified in a volume with a dimeter of 15 mm around the centerline. In NCCT images, voxels with signal density above 530 Hounsfield units were considered as calcification [19]. In the non-inverted PDIP-SOS MR images, a threshold of mean minus three times the standard deviation was used to define calcification.

Statistical Analysis

Statistical analyses were performed using MedCalc 13.2.2 (MedCalc Software, Ostend, Belgium). The Kolmogorov-Smirnov test was used to assess normal distribution of the continuous data. Continuous variables were reported as mean ± standard deviation, and categorical variables as absolute frequencies and proportions. Differences in diagnostic image quality ratings were assessed by averaging the four-point score provided by the two readers and then comparing QISS MRA and CTA, as well as PDIP-SOS and NCCT, using the Mann-Whitney U test. The same test was used to compare diagnostic confidence ratings between the two MRI reading sessions (QISS MRA only vs. QISS MRA with PDIP-SOS MRI). Agreement regarding the ratings was evaluated using linearly weighted Kappa-statistics with the level of agreement as follows: poor, $\kappa<0.20$; fair, $\kappa=0.21–0.40$; moderate, $\kappa=0.41–0.60$; good, $\kappa=0.61–0.80$; and excellent, $\kappa>0.80$. κ-values were reported with 95% confidence intervals (CI).

Difference and correlation in significant stenosis detection rate between QISS MRA, QISS MRA with PDIP-SOS MRI, and CTA were analyzed using the McNemar test and Kappa-statistics with the level of agreement as described above. Sensitivity, specificity, and accuracy were calculated on a per-segment basis. Agreement regarding the detection of stenosis between readers was also assessed using Kappa-statistics. Receiver Operating Characteristic (ROC) curve analysis was used to calculate area under the curve (AUC), presented with 95% confidence intervals. The DeLong method was used for pairwise comparison of ROC curves to determine significant differences between AUCs.

The difference in the segment-based presence of vascular calcification was analyzed with the McNemar test. Intraclass correlation coefficient (ICC) was used to evaluate inter-reader agreement and the difference in calcium volume quantified by NCCT and PDIP-SOS MRI was assessed using two-tailed paired samples t-test, Pearson's correlation and Bland-Altman analysis. Significant difference was considered at p-values less than 0.05.

Results

Our study population consisted of 26 patients (mean age: 70±8 years; range: 52–85 years), including 15 men (mean age: 71±8 years; range: 59–85 years) and 11 women (mean age: 69±8 years; range: 52–80 years). Eight patients were scanned at 1.5T and 18 patients at 3T. Further characteristics of the patient population are detailed in Table 2, and representative clinical cases at 1.5T and 3T are shown in Figures 1 and 2, respectively.

MRA and CTA examinations were performed on the same day in 22 (84.6%) cases, resulting in an average time gap between MRA and CTA of 1.5 days (min 0, max 12 days). DSA was performed within an average of 12.1 days (min 3, max 26 days) after MRA and 13.6 days (min 3, max 29 days) after CTA. The total acquisition time at 1.5 and 3T were 24±3 and 26.5 min, respectively. The average volume CT dose index of NCCT and CTA were 3.9±1.4 mGy and 4.0±1.0 mGy, respectively, while the average dose length product was 560.2±194.6 mGy · cm and 553.7±158.2 mGy · cm.

Out of 468 vascular segments, all four modalities (QISS MRA, PDIP-SOS MRI, CTA, and DSA) were available in 207 (44.2%) segments. Overall subjective image quality ratings were significantly higher for CTA (p=0.0369) and NCCT (p=0.0093), with moderate to excellent inter-reader agreement (all κ>0.517, Table 3).

Of the 207 segments, ≥50% stenosis was detected by QISS MRA, QISS MRA with PDIP-SOS, CTA, and DSA in 109 (52.7%), 105 (50.7%), 108 (52.5%), and 103 (49.8%) segments, respectively. No significant difference (all p>0.0971) and good to excellent agreement in significant stenosis detection rate was shown between the modalities (all κ>0.622; Table 4). Agreement in stenosis detection rate using non-contrast QISS MRA compared to CTA and DSA improved when calcification visualization was provided to the readers. The sensitivity, specificity and accuracy for the detection of ≥50% stenosis by the investigated techniques are shown in Table 5. An increase was observed in both sensitivity and specificity when PDIP-SOS was added to the protocol, resulting in a significantly improved diagnostic accuracy (p=0.0366) that is more comparable to CTA. Inter-reader agreement regarding the detection of significant vascular stenosis was excellent (all κ>0.832; Table 5).

Calcification was visualized by PDIP-SOS MRI and NCCT in 123 (59.4%) and 126 (60.8%) vascular segments, respectively (p=0.2500). Inter-reader assessment for the detection of vascular calcification showed excellent agreement for both PDIP-SOS and NCCT (ICC 0.910 [95% CI 0.882–0.932] and 0.940 [0.922–0.955], respectively). Quantification of calcification showed statistical difference between PDIP-SOS and NCCT (80.6±31.2mm^3 vs 88.0±29.8mm^3; p=0.0002) with high correlation between the techniques (r=0.77, p<0.0001; Figure 3). Bland-Altman analysis revealed an underestimation (mean of differences at −7.4mm^3) by PDIP-SOS MRI with the majority of data points within the limits of agreement (Figure 3).

Discussion

In this prospective study we investigated whether the addition of PDIP-SOS-based visualization of arterial wall calcification to non-contrast QISS MRA improved the diagnostic accuracy for PAD. This study illustrates that the visualization of lower-extremity vascular calcification improves the diagnostic accuracy of QISS MRA in detecting significant (≥50%) vascular stenosis in patients with PAD. Both sensitivity and specificity of QISS MRA improved and accuracy reached that of CTA when calcification visualization was provided to the readers.

Image quality was subjectively rated by two experienced observers in this study, and QISS MRA was found to provide similar diagnostic confidence as CTA. The major factors contributing to insufficient vascular delineation and increased image noise/artifacts that rendered a segment non-diagnostic on QISS MRA were the presence of intravascular stents and poor signal-to-noise ratio. In the CTA datasets, the major source of non-diagnostic segments was the presence of heavy calcification causing blooming artifact and suboptimal opacification.

The diagnostic accuracy of non-contrast QISS MRA evaluated here against DSA showed a sensitivity and specificity of 85% and 90%, respectively. The sensitivity and specificity of QISS MRA in the detection of ≥50% stenosis were improved (92% and 93%, respectively) when PDIP-SOS MRI-based calcification data were provided to the readers. The accuracy results obtained by the combined QISS MRA / PDIP-SOS MRI are in good agreement with that measured by CTA in this study and with accuracy data reported by others [20], or slightly lower compared to studies using non-invasive contrast-enhanced MRA as a reference standard [21; 22]. The specificity of our combined non-contrast MR protocol for the detection of significant arterial stenosis in the lower extremities was high in this study. Moreover, it is better than that generally reported for other non-contrast MRA techniques, such as subtractive 3D fast spin echo MRA [23]. The detection rate showed good to excellent agreement between the techniques and the inter-reader agreement for significant stenosis was excellent for all modalities.

Quantification of arterial wall calcifications by PDIP-SOS MRI showed a slight underestimation of the calcium volume compared to NCCT. Such discrepancy has been reported by previous studies using similar imaging techniques [15]. This discrepancy might represent an overestimation of lesion size by NCCT due to blooming artifact [4]. Unfortunately, an independent reference standard for calcium volume quantification is not available.

There has been an increasing interest in exploring the use of MR-based techniques for the visualization and quantification of arterial wall calcification. A high resolution ultra-short echo time (UTE) pulse sequence was found to be accurate for the quantification of plaque volumes and calcium density in endarterectomy samples [24]. A similar UTE sequence provided close correspondence in morphologic appearance of carotid plaque samples compared to micro-CT [25]. More recently, the feasibility of projection MRI using dual-echo 3D gradient-echo and 3D “point-wise encoding time reduction with radial acquisition” (PETRA) UTE pulse sequences have been demonstrated for the depiction of vascular calcification in patients with iliofemoral PAD [26]. While such prototype techniques are promising, they have significant practical limitations that have precluded widespread use for imaging of vascular calcifications. The PDIP-SOS MRI technique was designed to address such limitations and has been shown to outperform both 3D gradient echo and PETRA techniques for the visualization of vascular calcium in PAD patients [14]. The isotropic spatial resolution of the PDIP-SOS technique provides optimal image quality for the accurate localization and volume quantification of vascular calcifications. It has also been demonstrated that the PDIP-SOS technique is relatively insensitive to bowel and respiratory

motion in the abdominal region, and can visualize aorto-iliac and iliofemoral calcifications simultaneously [15].

While visualizing calcification *in vivo* is a promising MRI application, there is a practical benefit that CTA offers, but MRI still has to address. Calcified plaques are visualized along the angiogram with CTA, which allows for the evaluation of vascular lumen, stenosis, and plaque simultaneously. Using the MRI protocol we investigated here, the angiogram and vascular calcification are visualized in two separate datasets which may be more challenging to synthesize, especially if the 2D angiogram and the 3D calcification volume are not perfectly aligned. A recently proposed solution to this issue offers co-registration and fusion of the two datasets that potentially allows for more complete and more accurate MRI-based vascular evaluation [27].

This study has some limitations. The size of the cohort was relatively small and further multi-center studies may be necessary to confirm the diagnostic performance of this combined MRI protocol across a wider range of patients, indications, and clinical scenarios. Although the maximum time interval between the imaging studies was kept as short as feasible, disease progression during this time period may have occurred, that we were not able to capture from medical records and patient interviews. Objective image quality analysis was not performed as the QISS technique involves parallel imaging which makes the measurement of image noise and consequently the calculation of objective image quality measures unsuitable [28]. We also did not evaluate vascular lesions based on the Inter-Society Consensus for the Management of Peripheral Arterial Disease (TASC-II) classification [29] that has been used for treatment planning, due to the current trends towards the “endovascular first” approach [30]. While CTAs were performed in dual energy mode which allows for the generation of virtual non-contrast (VNC) images, our clinical protocol included a separate NCCT scan as the prototype VNC post-processing algorithms were not clinically used at the time of this study. Using VNC instead of NCCT images for calcification evaluation will substantially reduce radiation exposure in future studies. Finally, PDIP-SOS MRI is a 3D acquisition which does not provide full coverage of the entire lower extremity runoff, thus multiple acquisitions are needed if more than one region need to be visualized. Accordingly, we reported diagnostic accuracy results in our cohort only in a subset of segments in which all techniques were available.

In conclusion, the visualization of lower extremity PDIP-SOS-based arterial wall calcification improved the diagnostic accuracy of non-contrast QISS-MRA in detecting significant vascular stenoses. Quantification of vascular calcium with MRI showed good agreement with CTA. Based on our promising initial results, this combined protocol may prove especially useful for the comprehensive assessment of vascular anatomy prior to interventional procedure planning.

Acknowledgments

1. Funding

This study was supported by a research grant from Siemens and by NIH NHLBI R01 HL130093 (RRE).

3. Conflict of Interest:

The authors of this manuscript declare relationships with the following companies: U. Joseph Schoepf is a consultant for and / or receives research support from Astellas, Bayer, Elucid Bioimaging, Guerbet, HeartFlow Inc., and Siemens Healthcare. Akos Varga-Szemes receives institutional research and travel support from Siemens Healthcare and is a consultant for Elucid Bioimaging. Robert R. Edelman receives grant support and royalties from Siemens Healthcare. Ioannis Koktzoglou receives research support from Siemens Healthcare.

Abbreviations

ABI	ankle brachial index
CI	confidence interval
ICC	intraclass correlation coefficient
MIP	maximum intensity projection
NCCT	non-contrast computed tomography
PAD	peripheral artery disease
PDIP-SOS	proton density-weighted, in-phase stack-of-stars
PETRA	point-wise encoding time reduction with radial acquisition
QISS	quiescent interval slice-selective
UTE	ultra-short echo time
VNC	virtual non-contrast

References

1. Criqui MH, Aboyans V (2015) Epidemiology of peripheral artery disease. Circ Res 116:1509–1526 [PubMed: 25908725]
2. Hiatt WR, Hoag S, Hamman RF (1995) Effect of diagnostic criteria on the prevalence of peripheral arterial disease. The San Luis Valley Diabetes Study. Circulation 91:1472–1479 [PubMed: 7867189]
3. Pollak AW, Norton PT, Kramer CM (2012) Multimodality imaging of lower extremity peripheral arterial disease: current role and future directions. Circ Cardiovasc Imaging 5:797–807 [PubMed: 23169982]
4. Ouwendijk R, Kock MC, van Dijk LC, van Sambeek MR, Stijnen T, Hunink MG (2006) Vessel wall calcifications at multi-detector row CT angiography in patients with peripheral arterial disease: effect on clinical utility and clinical predictors. Radiology 241:603–608 [PubMed: 16966479]
5. Davenport MS, Khalatbari S, Cohan RH, Dillman JR, Myles JD, Ellis JH (2013) Contrast material-induced nephrotoxicity and intravenous low-osmolality iodinated contrast material: risk stratification by using estimated glomerular filtration rate. Radiology 268:719–728 [PubMed: 23579046]
6. Mathur M, Jones JR, Weinreb JC (2020) Gadolinium Deposition and Nephrogenic Systemic Fibrosis: A Radiologist's Primer. Radiographics 40:153–162 [PubMed: 31809230]
7. American College of Rardiology Committee on Drugs and Contrast Media. ACR Manual on Contrast Media. Available at: https://www.acr.org/-/media/ACR/Files/Clinical-Resources/Contrast_Media.pdf. Accessed June 3, 2020.
8. Tranche-Iparraguirre S, Marin-Iranzo R, Fernandez-de Sanmamed R, Riesgo-Garcia A, Hevia-Rodriguez E, Garcia-Casas JB (2012) Peripheral arterial disease and kidney failure: a frequent association. Nefrologia 32:313–320 [PubMed: 22508143]

9. Edelman RR, Sheehan JJ, Dunkle E, Schindler N, Carr J, Koktzoglou I (2010) Quiescent-interval single-shot unenhanced magnetic resonance angiography of peripheral vascular disease: Technical considerations and clinical feasibility. Magn Reson Med 63:951–958 [PubMed: 20373396]
10. Varga-Szemes A, Wichmann JL, Schoepf UJ et al. (2017) Accuracy of Noncontrast Quiescent-Interval Single-Shot Lower Extremity MR Angiography Versus CT Angiography for Diagnosis of Peripheral Artery Disease: Comparison With Digital Subtraction Angiography. JACC Cardiovasc Imaging 10:1116–1124 [PubMed: 28109932]
11. Hodnett PA, Ward EV, Davarpanah AH et al. (2011) Peripheral arterial disease in a symptomatic diabetic population: prospective comparison of rapid unenhanced MR angiography (MRA) with contrast-enhanced MRA. AJR Am J Roentgenol 197:1466–1473 [PubMed: 22109304]
12. Amin P, Collins JD, Koktzoglou I et al. (2014) Evaluating peripheral arterial disease with unenhanced quiescent-interval single-shot MR angiography at 3 T. AJR Am J Roentgenol 202:886–893 [PubMed: 24660721]
13. Altaha MA, Jaskolka JD, Tan K et al. (2017) Non-contrast-enhanced MR angiography in critical limb ischemia: performance of quiescent-interval single-shot (QISS) and TSE-based subtraction techniques. Eur Radiol 27:1218–1226 [PubMed: 27352087]
14. Ferreira Botelho MP, Koktzoglou I, Collins JD et al. (2017) MR imaging of iliofemoral peripheral vascular calcifications using proton density-weighted, in-phase three-dimensional stack-of-stars gradient echo. Magn Reson Med 77:2146–2152 [PubMed: 27297954]
15. Serhal A, Koktzoglou I, Aouad P et al. (2018) Cardiovascular magnetic resonance imaging of aorto-iliac and ilio-femoral vascular calcifications using proton density-weighted in-phase stack of stars. J Cardiovasc Magn Reson 20:51 [PubMed: 30078377]
16. Fleischmann D, Kamaya A (2009) Optimal vascular and parenchymal contrast enhancement: the current state of the art. Radiol Clin North Am 47:13–26 [PubMed: 19195531]
17. Fraioli F, Catalano C, Napoli A et al. (2006) Low-dose multidetector-row CT angiography of the infra-renal aorta and lower extremity vessels: image quality and diagnostic accuracy in comparison with standard DSA. Eur Radiol 16:137–146 [PubMed: 15988586]
18. Schneider CA, Rasband WS, Eliceiri KW (2012) NIH Image to ImageJ: 25 years of image analysis. Nat Methods 9:671–675 [PubMed: 22930834]
19. Bischoff B, Kantert C, Meyer T et al. (2012) Cardiovascular risk assessment based on the quantification of coronary calcium in contrast-enhanced coronary computed tomography angiography. Eur Heart J Cardiovasc Imaging 13:468–475 [PubMed: 22166591]
20. Wagner M, Knobloch G, Gielen M et al. (2015) Nonenhanced peripheral MR-angiography (MRA) at 3 Tesla: evaluation of quiescent-interval single-shot MRA in patients undergoing digital subtraction angiography. Int J Cardiovasc Imaging 31:841–850 [PubMed: 25697720]
21. Hodnett PA, Koktzoglou I, Davarpanah AH et al. (2011) Evaluation of peripheral arterial disease with nonenhanced quiescent-interval single-shot MR angiography. Radiology 260:282–293 [PubMed: 21502384]
22. Klasen J, Blondin D, Schmitt P et al. (2012) Nonenhanced ECG-gated quiescent-interval single-shot MRA (QISS-MRA) of the lower extremities: comparison with contrast-enhanced MRA. Clin Radiol 67:441–446 [PubMed: 22142498]
23. Ward EV, Galizia MS, Usman A, Popescu AR, Dunkle E, Edelman RR (2013) Comparison of quiescent inflow single-shot and native space for nonenhanced peripheral MR angiography. J Magn Reson Imaging 38:1531–1538 [PubMed: 23564638]
24. Sharma S, Boujraf S, Bornstedt A et al. (2010) Quantification of calcifications in endarterectomy samples by means of high-resolution ultra-short echo time imaging. Invest Radiol 45:109–113 [PubMed: 20065858]
25. Du J, Corbeil J, Znamirowski R et al. (2011) Direct imaging and quantification of carotid plaque calcification. Magn Reson Med 65:1013–1020 [PubMed: 21413065]
26. Edelman RR, Flanagan O, Grodzki D, Giri S, Gupta N, Koktzoglou I (2015) Projection MR imaging of peripheral arterial calcifications. Magn Reson Med 73:1939–1945 [PubMed: 24957402]

27. Serhal A, Koktzoglou I, Edelman RR (2019) Feasibility of Image Fusion for Concurrent MRI Evaluation of Vessel Lumen and Vascular Calcifications in Peripheral Arterial Disease. AJR Am J Roentgenol 212:914–918 [PubMed: 30714829]

28. Dietrich O, Raya JG, Reeder SB, Reiser MF, Schoenberg SO (2007) Measurement of signal-to-noise ratios in MR images: influence of multichannel coils, parallel imaging, and reconstruction filters. J Magn Reson Imaging 26:375–385 [PubMed: 17622966]

29. Norgren L, Hiatt WR, Dormandy JA et al. (2007) Inter-Society Consensus for the Management of Peripheral Arterial Disease (TASC II). J Vasc Surg 45 Suppl S:S5–67 [PubMed: 17223489]

30. Lin JH, Brunson A, Romano PS, Mell MW, Humphries MD (2019) Endovascular-First Treatment Is Associated With Improved Amputation-Free Survival in Patients With Critical Limb Ischemia. Circ Cardiovasc Qual Outcomes 12:e005273 [PubMed: 31357888]

Key points:

1. Agreement in stenosis detection rate using non-contrast quiescent-interval slice-selective MRA compared to DSA improved when calcification visualization was provided to the readers
2. An increase was observed in both sensitivity and specificity for the detection of ≥50% stenosis when MRI-based calcification assessment was added to the protocol, resulting in a diagnostic accuracy more comparable to CTA
3. Quantification of calcification showed statistical difference between MRI and non-contrast CT, however, a high correlation was observed between the techniques

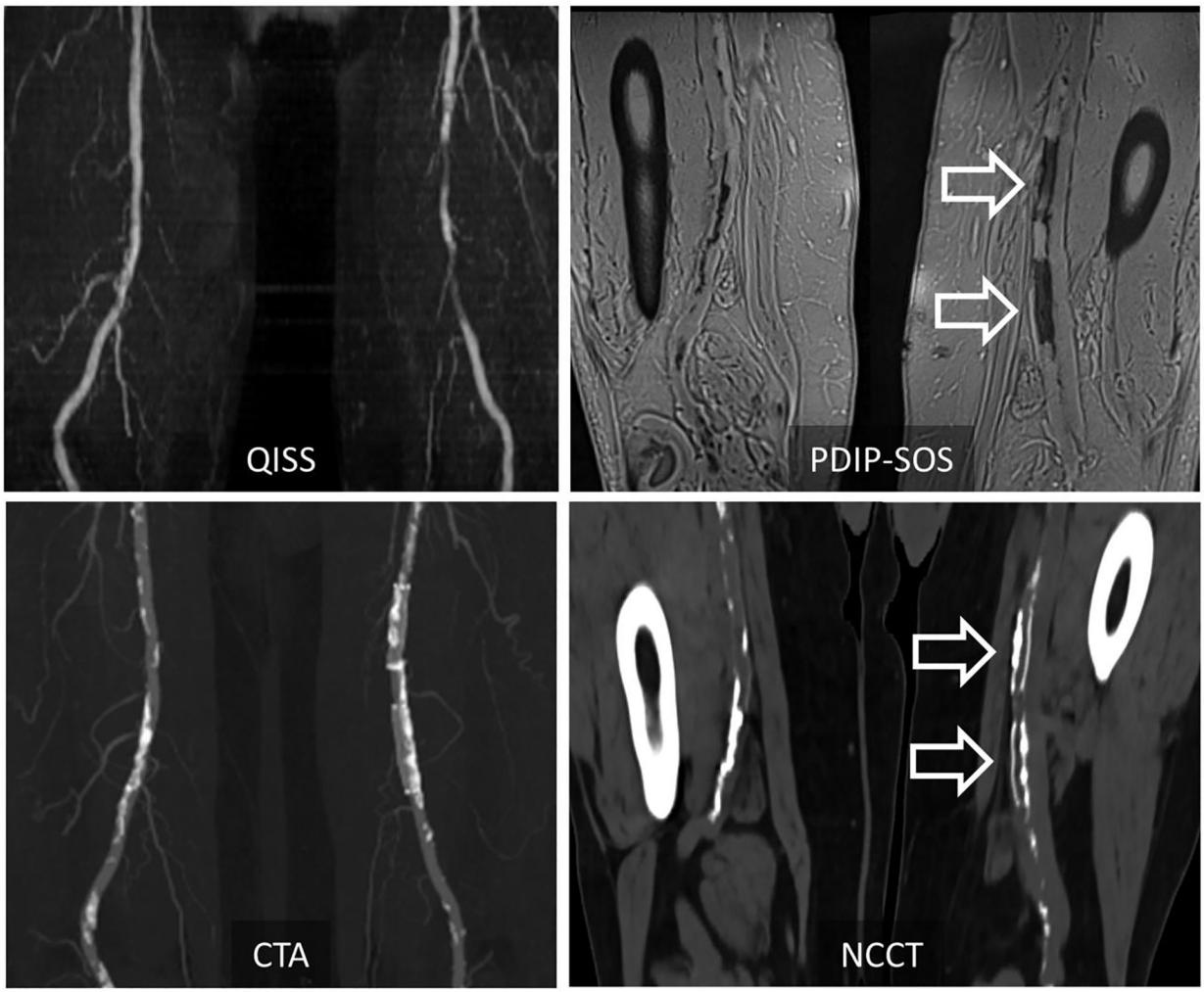

Figure 1 –.

Representative case in a 72-year-old man with peripheral artery disease at 1.5T. PDIP-SOS MRI shows low-signal calcification involving the right superficial femoral artery, as well as two intra-vascular stents in the left superficial femoral artery (arrows). Corresponding non-contrast CT and contrast enhanced CTA shows good visual correlation in the location of vascular calcification between the two modalities. Calcification, however, appears to be more extensive on CT, possibly due to blooming artifacts. QISS MRA is also shown for comparison's sake. PDIP-SOS, proton density weighted, in-phase 3D stack-of-stars; QISS, quiescent interval slice-selective

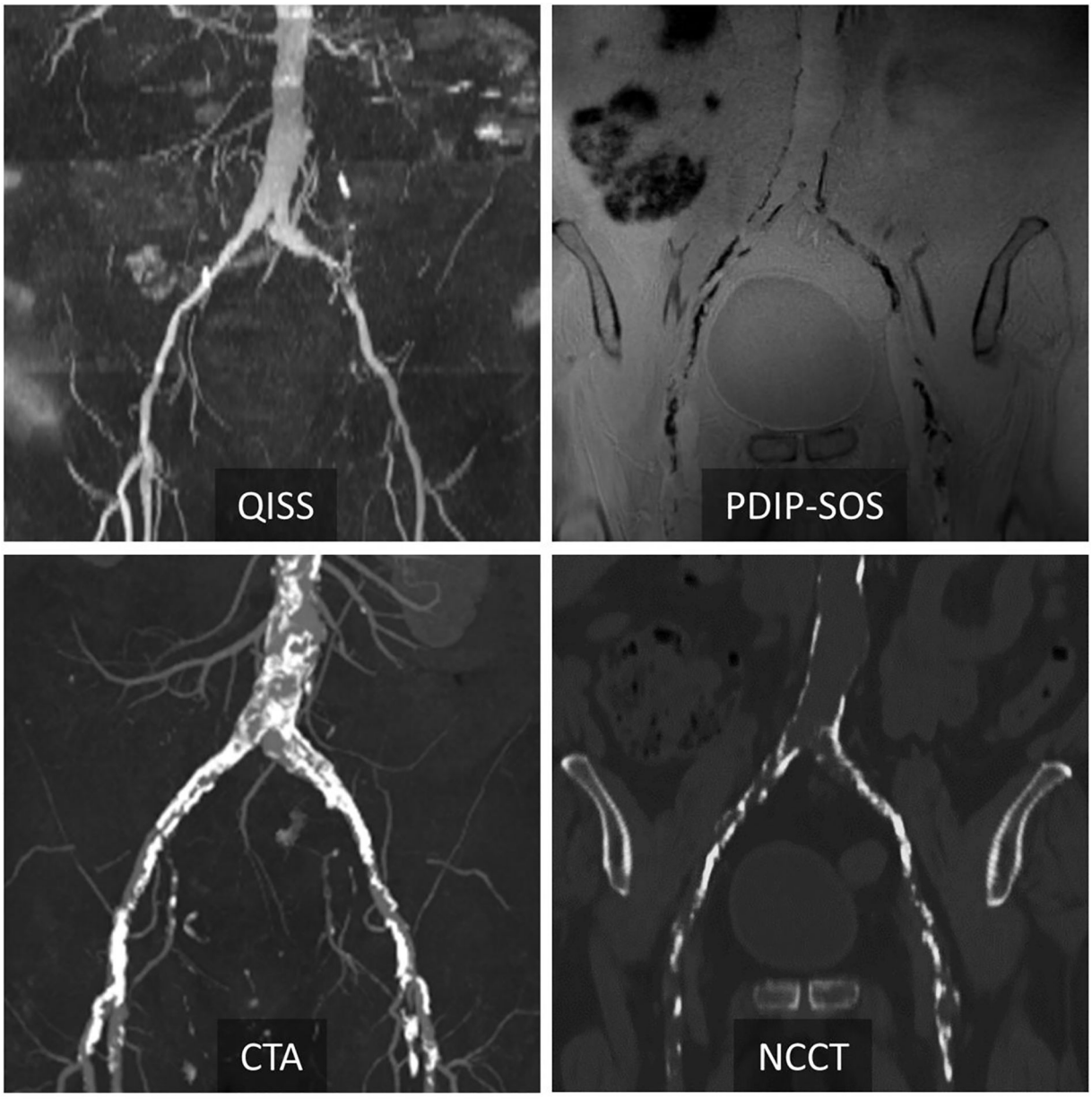

Figure 2 –.

Representative case in a 77-year-old man with peripheral artery disease at 3T. Corresponding QISS MRA and CTA show peripheral artery disease in the common iliac arteries. PDIP-SOS MRI indicates extensive low-signal calcification involving the distal aorta, bilateral common and external iliac arteries. There is excellent correspondence in the location and extent of calcification between PDIP-SOS MRI and non-contrast CT (NCCT). PDIP-SOS, proton density weighted, in-phase 3D stack-of-stars; QISS, quiescent interval slice-selective

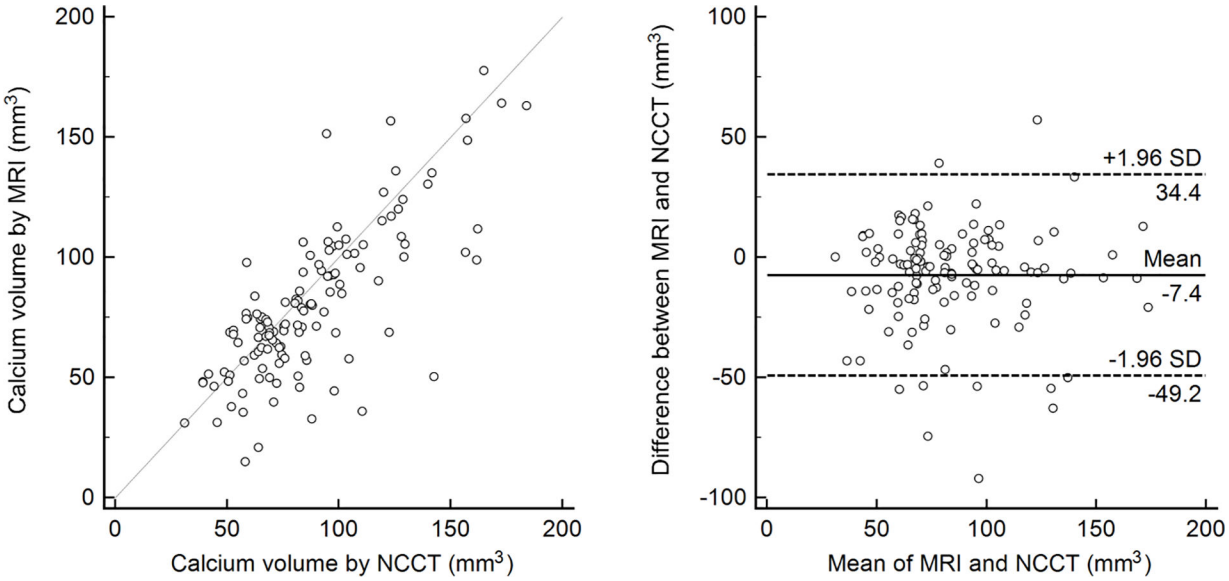

Figure 3 –.

Correlation between PDIP-SOS and NCCT-based calcification assessment. Scatter plot shows significant correlation (r=077, P<0.0001) between PDIP-SOS and NCCT based vascular calcium quantification. Bland-Altman analysis indicates good agreement in vascular calcium quantification between PDIP-SOS and NCCT with a −7.4mm^3 underestimation by the MRI technique. PDIP-SOS, proton density weighted, in-phase 3D stack-of-stars; NCCT, non-contrast computed tomography

Table 1 –

Pulse sequence parameters

	QISS MRA		PDIP-SOS	
	1.5T	**3T**	**1.5T**	**3T**
Imaging type	2D	2D	3D	3D
Field of view (mm)	400 × 400	400 × 400	410 × 410	416 × 416
Slice thickness (mm)	3	3	0.5	0.5
In-plane resolution (mm)	1.0 × 1.0	1.0 × 1.0	1.0 × 1.0	1.1 × 1.1
Echo time (ms)	1.4	1.7	4.7	2.5
Repetition time (ms)	3.5	3.8	9.6	5.0
Flip angle	90°	90°	4.5°	2.5°
Bandwidth (Hz/pixel)	658	960	300	750
Inversion time (ms)	350	350		
GRAPPA	2	2		
Readout	Cartesian	Cartesian	Stack-of-Stars	Stack-of-Stars
Acquisition time (min)	12*	12*	6.2	5.9

GRAPPA, generalized autocalibrating partially parallel acquisition acceleration factor

Stack-of-stars denotes radial acquisition within each slice-encoding step, and Cartesian sampling in the slice-encoding direction

*Considering 10 stations, a heart rate of 70 beats per minute, and 15 seconds breath-holds in the 3 abdominal stations

Table 2 –

Patient characteristics Data are displayed as mean ± standard deviation or frequency (%)

Age (year)	70 ± 8
Gender (male)	15 (57.6%)
Race	
African American	10 (38.4%)
Caucasian	16 (61.5%)
Weight (kg)	84.7 ± 18.0
Height (cm)	169.2 ± 11.4
Body Mass Index (kg/m^2)	30.0 ± 5.5
Ankle brachial index	0.67 ± 0.2
Diabetes mellitus	13 (50.0%)
Hypertension	23 (88.4%)
Dyslipidemia	23 (88.4%)
Lower leg stent	7 (26.9%)
Known coronary artery disease	18 (69.2%)
Prior myocardial infarction	2 (11.5%)
Prior transient ischemic attack	8 (30.7%)

Table 3 –

Subjective image quality ratings and inter-reader agreement

	CTA	QISS MRA	*p*-value	NCCT	PDIP-SOS	*p*-value
Rating	4.0 [3.0–4.0]	3.0 [3.0–4.0]	0.0369	4.0 [4.0–4.0]	4.0 [3.0–4.0]	0.0093
κ	0.819 [0.778–0.860]	0.669 [0.605–0.733]		0.891 [0.846–0.924]	0.517 [0.401–0.632]	

CTA, Computed tomography angiography; QISS MRA, Quiescent interval slice-selective magnetic resonance angiography; NCCT, non-contrast CT; PDIP-SOS, proton density-weighted in-phase stack of stars MR

Results are reported with [95% confidence interval]

Table 4 –

Agreement in stenosis detection rate among the techniques

Modalities	κ	95% CI	*p*-value*
QISS MRA / CTA	0.622	0.515–0.729	0.0971
QISS MRA / DSA	0.758	0.669–0.847	0.1244
QISS MRA with PDIP-SOS / CTA	0.816	0.737–0.894	0.6476
QISS MRA with PDIP-SOS / DSA	0.855	0.784–0.925	0.3018
CTA / DSA	0.845	0.772–0.918	0.4545

CTA, Computed tomography angiography; QISS MRA, Quiescent interval slice-selective magnetic resonance angiography; PDIP-SOS, proton density-weighted in-phase stack of stars; DSA, digital subtraction angiography; CI, confidence interval

*Indicates difference in detection rate by the McNemar test

Table 5 –

Sensitivity, specificity, diagnostic accuracy and inter-reader agreement Per-segment sensitivity, specificity, and diagnostic accuracy of QISS MRA with and without PDIP-SOS MRI and CTA for the detection of hemodynamically significant (≥50%) stenosis compared with DSA, as well as inter-reader agreement in stenosis detection (κ)

	Sensitivity (%)	95% CI	Specificity (%)	95% CI	AUC	95% CI	κ	95% CI
CTA	90.2 (93/103)	82.8–95.2	94.2 (98/104)	87.8–97.8	0.923	0.877–0.955	0.901	0.849–0.953
QISS MRA	85.4 (88/103)	77.1–91.6	90.3 (94/104)	83.0–95.2	0.879	0.827–0.920	0.832	0.756–0.908
QISS MRA with PDIP-SOS	92.2 (95/103)	85.2–96.5	93.2 (97/104)	86.6–97.2	0.928	0.883–0.959	0.855	0.786–0.925

Sensitivity and specificity values are % (n/N)

CTA, Computed tomography angiography; QISS MRA, Quiescent interval slice-selective magnetic resonance angiography; PDIP-SOS, proton density-weighted in-phase stack of stars; DSA, digital subtraction angiography; CI, confidence interval; AUC, area under the curve